



0006-2952(94)E0140-G

INHIBITION OF PURINE NUCLEOBASE TRANSPORT IN HUMAN ERYTHROCYTES AND CELL LINES BY PAPAVERINE

INVESTIGATION OF STRUCTURE–ACTIVITY RELATIONSHIP

MARTIN KRAUPP,* BARBARA PASKUTTI, CLAUDIA SCHÖN and RICHARD MARZ

Institut für Medizinische Chemie der Universität Wien, Währingerstr. 10, A-1090 Vienna, Austria

(Received 29 October 1993; accepted 18 March 1994)

Abstract—Papaverine was found to be an effective inhibitor of hypoxanthine transport not only in human erythrocytes, but also in the human cell lines HL60 (myeloid) and U937 (monocytic). IC_{50} values for inhibition of hypoxanthine influx ranged from 6 to 20 μ M. In erythrocytes papaverine was found to be a non-competitive inhibitor of hypoxanthine equilibrium-exchange transport with a K_i value of ≈ 13 μ M, which is in close agreement with the respective IC_{50} values estimated for *zero-trans* influx of hypoxanthine. In addition papaverine also had a slight inhibitory effect on unmediated nucleobase transport, most likely due to a perturbation of the membrane lipid environment. Several papaverine analogs were tested for their inhibitory effect on nucleobase transport. Only ethaverine was as effective as papaverine. Drotaverine and berberine were moderately inhibitory while laudanospine had no inhibitory effect at all. Isoquinoline acted as a very weak inhibitor.

Key words: erythrocytes; HL60 cells; U937 cells; nucleobase transport; papaverine; inhibition kinetics

In mammalian cells nucleotides are synthesized either *de novo* or from exogenous nucleosides and bases (salvage pathway). Two obligatory biochemical events are involved in the salvage of purine bases in mammalian cells: transport across the plasma membrane and subsequent intracellular conversion to the respective purine nucleoside monophosphates [1–3]. The transport step has attracted interest since nucleoside transport inhibitors can enhance the effectiveness of various antimetabolites, such as 5'-fluorouracil [4], 2'-deoxyadenosine [5], and methotrexate [6, 7] by inhibiting either purine/pyrimidine salvage [8–10] or drug efflux [11].

Recent research has centred on the nucleoside carrier and little is known about the transport of nucleobases in human cells and its modulation by inhibitors. Nucleobase transport in fact plays an equally important role in purine salvage and thus might be an interesting target for the modulation of this salvage by pharmacological agents.

Two distinct mechanisms of carrier-mediated nucleobase transport have been described: (1) sodium-dependent nucleobase transport in epithelial cells [12] and (2) facilitated diffusion operating in non-epithelial cells. The facilitative carrier for nucleobases in human RBCs† has recently been characterized and found to be well described by the alternating conformation model for carrier-mediated transport [13, 14]. It preferentially transports purine bases, with adenine and guanine displaying the

highest affinity. Various studies have demonstrated that the base carrier in human cells tolerates bulky substituents on N⁹ of the purine ring, but has no affinity towards nucleosides and the nucleoside transport inhibitors dipyridamole and nitrobenzylthioinosine [15, 16], although the nucleoside dideoxyguanosine and acyclovir and ganciclovir, two nucleoside analogs, are substrates [17, 18].

Papaverine has been used clinically as a spasmolytic and vasodilating drug, due to its direct relaxing effect on smooth muscle [19]. In addition, it is among the few substances known to inhibit nucleobase transport in mammalian cells. Its inhibitory action on adenine transport in human platelets was found to be competitive [20], suggesting that papaverine interacts with the carrier substrate binding site. Besides nucleobase transport, papaverine is also known to inhibit nucleoside transport [21]. In spite of its low specificity as transport inhibitor, papaverine and other benzyl-isoquinoline-alkaloids offer an opportunity to characterize the nucleobase transporter substrate binding site. We therefore reinvestigated the kinetics of papaverine inhibition of nucleobase transport in erythrocytes using an inhibitor stop method to assay transport, which in the case of nucleobase transport is superior to the conventional oil stop techniques [13]. In addition, we also tested various commercially available papaverine analogues for their inhibitory effects on the nucleobase carrier in order to gain some information about structure inhibition relationships.

MATERIALS AND METHODS

Preparation of human RBCs. Recently outdated

* Corresponding author. Tel. (43) 1/3191484–223; FAX (43) 1/3107210.

† Abbreviations: FCS, fetal calf serum; RBC, red blood cell; IMP, inosinemonophosphate; PRPP, 5'-phosphoribosyl-1-pyrophosphate.

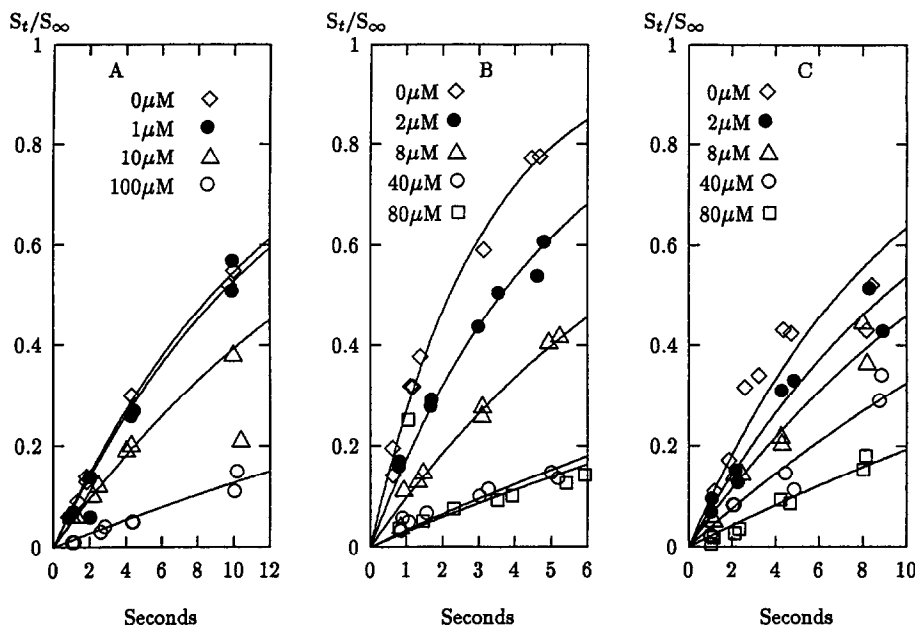


Fig. 1. Representative time courses of hypoxanthine influx into human erythrocytes (A), HL60 cells (B), U937 cells (C). Erythrocytes were preincubated at 25° with papaverine at the indicated concentrations at a hematocrit of 10% in HEPES buffered saline. HL60 and U937 cells were harvested in the log phase, washed and kept in buffered saline at 4° until the beginning of the experiment. Preincubation was also carried out at 25° at a cell density of $2\text{--}3 \times 10^7/\text{mL}$. Influx was started by mixing 10 μL of 500 μM [^3H]hypoxanthine with 90 μL of cell suspension and stopped by rapidly adding 700 μL of ice-cold papaverine stop solution. Processing of samples and calculation of initial transport rates was carried out as described in Materials and Methods.

blood was obtained from the bloodbank of the general hospital of the University of Vienna. Blood was mixed with an equal volume of saline and centrifuged at 3000 rpm. Supernate and buffy layer were removed and the pellet resuspended three times in at least 5 vol. of HEPES-buffered saline (NaCl 145 mM, HEPES 10 mM pH 7.4). The tube was rocked gently at room temperature for at least 10 min before centrifugation to ensure complete removal of endogenous purines (e.g. uric acid). The pellet obtained after the final wash was either resuspended in an equal volume of HEPES-buffered saline to give a hematocrit of 50% or used directly as "loosely packed cells".

Human cell lines. HL60 and U937 cells were cultivated in NaHCO_3 buffered RPMI-1640 medium containing 10% FCS, gassed with 5% CO_2 . Cells harvested in log-phase were washed with buffer [NaCl 130 mM, KH_2PO_4 1 mM, K_2HPO_4 2 mM, MgSO_4 1 mM, glucose 10 mM, HEPES 10 mM (pH 7.4)], resuspended in the same buffer to give a final density of $80\text{--}100 \times 10^6/\text{mL}$ and kept at 4° until the beginning of the experiment.

Transport measurements. Transport was assayed as recently described [14]. Incubation was started by mixing aliquots of cell suspension or packed cells and radioactive substrate under continuous vortexing in a 1.5 mL Eppendorf centrifuge tube at 25°. Total reaction volume was 100 μL . Transport was stopped by adding 700 μL of papaverine (20 mM) in saline cooled

in a freezing mixture to about -2° . Within 10 sec 0.2 mL of a mixture of dibutyl-phthalate/di-octylphthalate (4/1 by weight, density $\approx 1.035 \text{ g/cm}^3$) was added and the cells separated immediately from the medium by centrifugation through the oil. When transport was measured in erythrocytes, silicone oil was used instead. To measure unspecifically trapped radioactivity, cells, substrate and stop solution were mixed simultaneously and centrifuged through oil.

Time measurements. Incubation times were determined using an electronic clock (Breitenbach and Heller, Vienna, Austria) with a precision of 0.01 sec. The clock was started and stopped by microswitches attached to the plunger of the pipettes used to dispense the start and stop solutions.

Sample processing. Aliquots for radioactivity measurements were taken from the supernatant; the remainder was removed by suction and the tubes rinsed with H_2O . In the case of erythrocytes the cell pellet was hemolysed by adding 450 μL H_2O and extracted with perchloric acid (0.5 M final concn). Cell pellets obtained from cell lines were solubilized with NaOH/SDS (0.1 M/2%) and neutralized with HClO_4 . After centrifugation radioactivity in the clear supernate was measured by liquid scintillation counting in a Packard CA2000 counter (Packard Instruments) with a constant counting error of 1%.

Data analysis. Cell volume and extracellular space of cell pellets were determined with $^3\text{H}_2\text{O}$ and [^{14}C]-inulin [22].

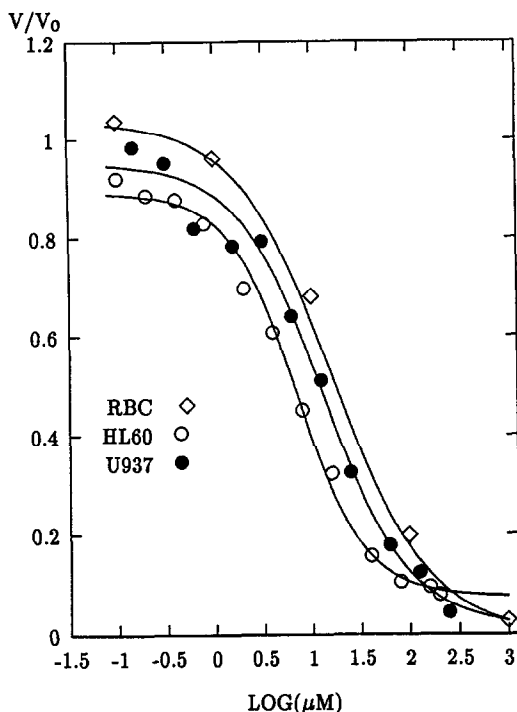


Fig. 2. Inhibition of hypoxanthine transport in human cells by papaverine. Erythrocytes (RBC), HL60 and U937 cells were preincubated as described for Fig. 1. Transport was assayed as described in Materials and Methods. The data shown are from independent representative experiments. At least two replicate experiments were carried out with similar results.

$$Y_t = Y_\infty [1 - \exp(kt)] \quad (1)$$

$$v = \frac{V_{\max}[S]}{K_m + [S]} + C[S] \quad (2)$$

$$v = \frac{V[S]}{K_S(1 + [I]/K_{i1}) + [S](1 + [I]/K_{i2})} \quad (3)$$

$$v = \frac{V_0(IC_{50})^n}{(IC_{50})^n + [I]^n} \quad (4)$$

Initial rates were obtained by fitting eqn 1 to time courses of influx of labelled substrates using non-linear least squares regression. Initial rates were calculated from the slopes at 0 seconds. When initial rate data obtained at a single papaverine concentration were analysed, the kinetic parameters V_{\max} , K_m and C were determined by non-linear least squares regression analysis using eqn 2. In the case of pooled data eqn 3 was fitted to obtain the parameters V , K_S , K_{i1} , K_{i2} . In this case the non-saturable flux component ($C[S]$) was subtracted before carrying out the regression analysis. Similarly, IC_{50} values were estimated by measuring initial rates in the presence of varying concentrations of inhibitor and fitting the logistic eqn 4 to these data. Non-linear least squares regression was conducted

using subroutine CURFIT, which is a Fortran implementation of Marquard's algorithm as described in Ref. 23.

Chemicals. [G - 3H]Hypoxanthine, 3H_2O and [^{14}C]inulin were purchased from Amersham (Amersham, U.K.). Papaverine-HCl, berberine, ethaverine-HCl, unlabeled nucleobases and purine analogs were obtained from the Sigma Chemical Co. (Poole, U.K.). Isoquinoline and laudanosine were provided by Aldrich (Milwaukee, WI, U.S.A.). Drotaverine was a generous gift from Dr Kopelet-Frank (Department of Pharmaceutical Chemistry, University of Vienna). Silicone oil AR200 (density $\approx 1.05 \text{ g/cm}^3$) was purchased from Wacker Chemie (Munich, F.R.G.). Dibutyl-phthalic acid and dioctyl-phthalic acid were obtained from Aldrich. Ready Solve scintillation cocktail was from Beckman Instruments.

RESULTS

Inhibition of hypoxanthine transport in human cells by papaverine

Figure 1 shows time courses of *zero-trans* influx of $50 \mu\text{M}$ hypoxanthine into erythrocytes, HL60 and U937 cells preequilibrated with various papaverine concentrations. It also illustrates our method of obtaining initial rates by fitting eqn 1 to the data. It has been shown by us and others [13, 14] that papaverine is a very efficient and rapid transport quencher in human erythrocytes. The data of Fig. 1 extend this observation to HL60 (myeloid) and U937 (monocytic) cells which are also derived from bone marrow. Influx is virtually equally rapid in erythrocytes and U937 cells with half times for transmembrane equilibration of about 10 sec at 25° , while influx into HL60 cells is significantly quicker ($t/2 \approx 2 \text{ sec}$).

In Fig. 2, initial rates measured in the presence of graded concentrations of papaverine are plotted as the fraction of control rates versus the logarithm of inhibitor concentration. The results obtained for erythrocytes (RBC) and the two human nonerythroid cell lines HL60 and U937 show that hypoxanthine transport is similarly sensitive to inhibition by papaverine in all three cell types examined. In all cases 100% inhibition was approached at concentrations near 1 mM, proving that the papaverine concentration used in the stop solution (20 mM) is sufficiently high to cause complete transport inhibition in all cell types. The rapidity of transport inhibition can also be deduced from the fact that cell-associated radioactivity at $t = 0$ seconds was equivalent to that calculated from the measured extracellular, i.e. inulin impermeable, space (data not shown).

The logistic eqn 4 was fitted by non-linear least squares regression to calculate IC_{50} values of papaverine. The IC_{50} values obtained for the data shown in Fig. 2 were $16 \mu\text{M}$ for erythrocytes, $6 \mu\text{M}$ for HL60 cells and $13 \mu\text{M}$ for U937 cells. Values for the parameter n which corresponds to the slope in Hill-plots ranged from 0.8 to 1.3. The fact that sensitivity to papaverine is similar in every respect suggests that papaverine interacts with only one single carrier type, and that very similar facilitative

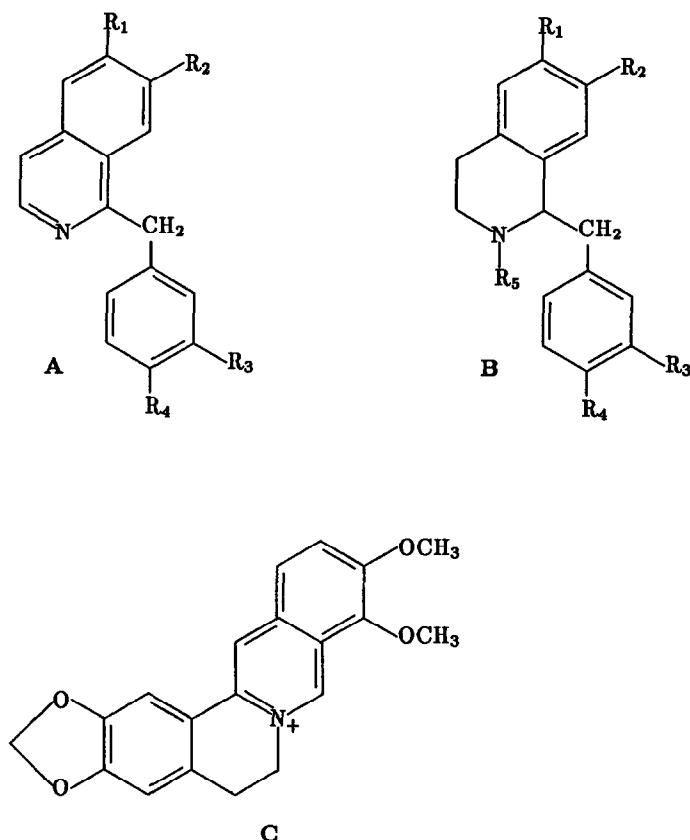


Fig. 3. Structures of papaverine analogs

	Compound	R ₁	R ₂	R ₃	R ₄	R ₅
A	Papaverine	CH ₃ O—	CH ₃ O—	CH ₃ O—	CH ₃ O—	
	Ethaverine	C ₂ H ₅ O—	C ₂ H ₅ O—	C ₂ H ₅ O—	C ₂ H ₅ O—	
B	Drotaverine	C ₂ H ₅ O—	C ₂ H ₅ O—	C ₂ H ₅ O—	C ₂ H ₅ O—	H
	Laudanosine	CH ₃ O—	CH ₃ O—	CH ₃ O—	CH ₃ O—	CH ₃ —
	Laudanosoline	—OH	—OH	—OH	—OH	CH ₃ —
C	Berberine					

nucleobase transport systems may operate in HL60 cells, U937 cells and erythrocytes (see Discussion). This assumption is further supported by the observation that in all three cell types hypoxanthine transport was resistant to inhibition by dipyradimole (data not shown).

Inhibition of hypoxanthine transport in erythrocytes by papaverine analogs

In order to characterize the carrier papaverine binding site, the inhibitory effects of various papaverine analogs on hypoxanthine influx into erythrocytes were measured. The structural formulae of the compounds used are shown in Fig. 3. Ethaverine, in which methylether is replaced by ethylether groups, is a very efficient inhibitor with a slightly higher affinity for the carrier as shown by its lower IC₅₀ value (Fig. 4). This suggests that affinity might correlate with the alkyl chain length of the

ether groups and is also consistent with the fact that drotaverine is at least a weak inhibitor, while laudanosine bearing methylether instead of ethylether groups has no inhibitory effect at all. Reduction of the aromatic isoquinoline nucleus to the respective tetrahydro form causes complete loss of inhibition (laudanosine) or at least a drastic reduction in affinity for the carrier (drotaverine). Isoquinoline *per se* is only a weak inhibitor of nucleobase transport (IC₅₀ ≥ 1500 μM).

Mechanism of inhibition by papaverine

The inhibitory mechanism of papaverine was further explored. The data of Fig. 5 show the results obtained from equilibrium exchange influx experiments with erythrocytes in the presence and absence of papaverine. In order to prevent intracellular phosphoribosylation of hypoxanthine to IMP, RBCs were washed and suspended in

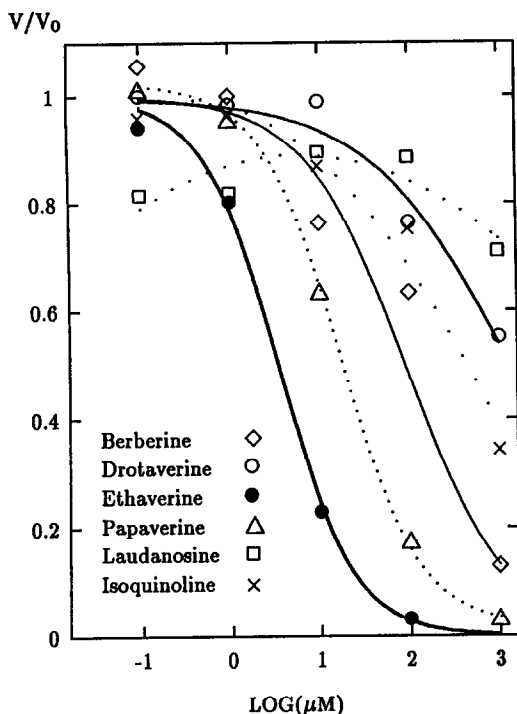


Fig. 4. Inhibition of hypoxanthine transport in erythrocytes by papaverine and papaverine analogs. Preparation of erythrocytes and transport assays were done as described for Fig. 1 and in Materials and Methods. The data shown are from independent representative experiments. At least two replicate experiments were carried out with similar results.

phosphate free HEPES buffered saline. This treatment minimizes synthesis of PRPP, the limiting co-substrate for this reaction, by PRPP-synthetase (EC 2.7.6.1). In addition preloading of cells with low concentrations of hypoxanthine (i.e. $<10 \mu\text{M}$) can be prevented since the K_m for hypoxanthine transport is approx. $100 \mu\text{M}$. It has been shown previously, that under these precautions hypoxanthine is not metabolized to any significant extent at 25° [14, 24]. Figure 5A demonstrates that at all papaverine concentrations equilibrium-exchange transport of hypoxanthine can be resolved into a saturable hyperbolic and an unsaturable linear component which is most likely due to diffusion through the lipid bilayer [14]. Kinetic parameters including the linear term were estimated by fitting eqn 2 to the data. After subtraction of the fitted linear component, the data conformed to simple Michaelis-Menten kinetics as shown by the linear double-reciprocal plots in Fig. 5B. The data also show that papaverine, while causing strong inhibition of saturable transport, also has a slight but measurable inhibitory effect on unsaturable (i.e. unmediated) transport (Table 1, Fig. 5A). Inspection of the double-reciprocal plots (Fig. 5B) demonstrates that papaverine causes a drastic reduction in the V_{\max} of transport but has no significant effect on K_m

values determined at the respective inhibitor concentrations (Table 1). It is therefore a true non-competitive inhibitor of nucleobase transport in human RBCs. When eqn 3 was fitted to the pooled data for all papaverine concentrations, the resulting values for K_{i1} and K_{i2} were not significantly different (Table 1). Therefore eqn 3 is in fact reduced to one describing non-competitive inhibition.

DISCUSSION

Transport of nucleobases occurs very rapidly. The data of Fig. 1 demonstrate the absolute necessity to measure flux rates in very short time intervals, (i.e. less than 2 sec). Although the transport system appears to be more active in HL60 cells than in erythrocytes and U937 cells, it is equally sensitive to inhibition by papaverine in all three cell types (Fig. 2) and equally resistant to inhibition by dipyrindamole, suggesting that the same or at least a similar transport system operates in all three cell types. Since the recently described active nucleobase transporter is sensitive to inhibition by dipyrindamole [12], our findings suggest that this type of transport is not active in human erythrocytes, HL60 cells and U937 cells.

Due to their hydrophobic character papaverine (partition coefficient octanol:H₂O > 20) as well as its analogs will readily diffuse through the cell membrane [21]. Since the compounds can thus not be confined to one side of the membrane the inhibitors were allowed to equilibrate across the membrane in all experiments. However, the type of inhibition observed in transport experiments also depends on whether the inhibitor binds to the carrier on the *cis*-side, the *trans*-side, or on both sides of the membrane. We therefore chose the equilibrium-exchange protocol, since it has been demonstrated that even when the inhibitor can not be confined to one compartment the true inhibitory mechanism is reliably revealed [25]. The kinetic data demonstrate that in contrast to previous results [20], papaverine inhibits carrier-mediated nucleobase transport in a purely non-competitive manner. Non-competitive inhibition by papaverine has also been observed with the transport of nucleosides, leading to the conclusion that nucleoside transport inhibition by papaverine results from an unspecific hydrophobic perturbation of the membrane lipid environment resulting in reduced carrier mobility [21].

Papaverine may cause a perturbation of the lipid environment within the membrane as shown by the weak inhibition of the unmediated flux component. However the data obtained with structural analogs of papaverine demonstrate that a structure inhibition relationship exists. Due to their aromatic ring systems, papaverine and ethaverine can assume a planar conformation which appears to facilitate binding to the carrier, while reducing the isoquinoline nucleus (drotaverine, laudanosine) to the tetrahydro form causes the loss of both the planar isoquinoline-ring conformation and of affinity. Thus the data suggest that inhibition of the carrier-mediated transport component is not the result of unspecific hydrophobic interaction but rather to a more specific interaction with the carrier.

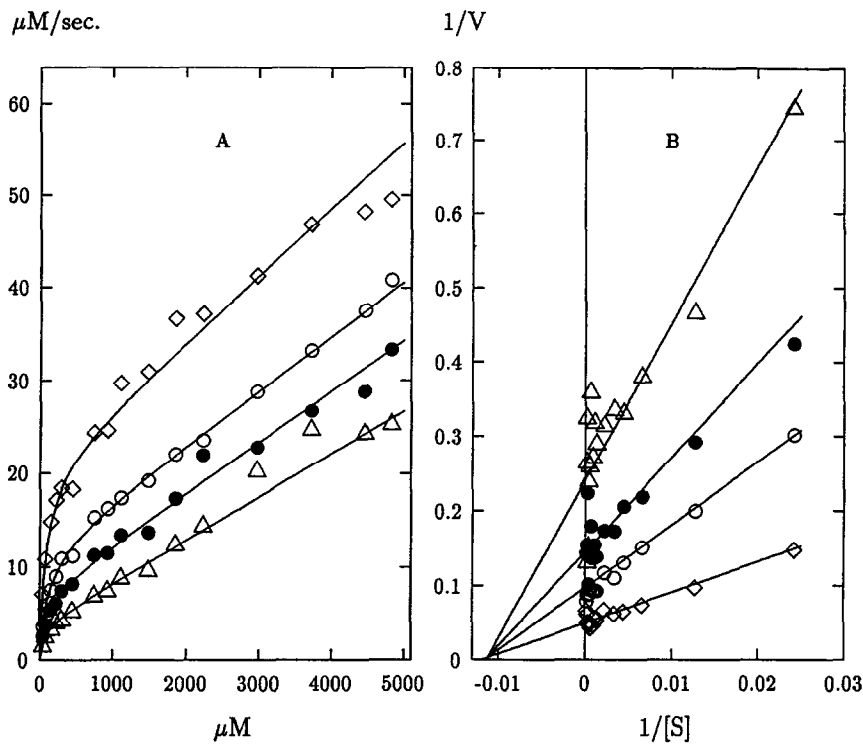


Fig. 5. Kinetics of hypoxanthine equilibrium-exchange transport in erythrocytes and inhibition by papaverine. For equilibrium-exchange transport, erythrocytes were suspended in HEPES buffered saline (hematocrit 50%) and pre-equilibrated at room temperature with unlabeled hypoxanthine \pm papaverine. Transport was measured by mixing 20 μL of cell suspension with 80 μL of labeled substrate (\pm papaverine). The chemical concentrations of hypoxanthine and papaverine were the same as in the cell suspension. All other procedures were carried out as described in Materials and Methods. Papaverine concentrations: (\diamond) 0 μM , (\circ) 12.5 μM , (\bullet) 25 μM , (\triangle) 50 μM . (A) Substrate velocity plot, (B) Double-reciprocal plot of the data after subtraction of the unsaturable flux component.

Table 1. Kinetic parameters of inhibition of hypoxanthine equilibrium-exchange transport by papaverine

Experiment	Papaverine (μM)	V_{\max} ($\mu\text{M}/\text{sec}$)	K_m (μM)	Const. ($\text{sec.}^{-1}10^{-3}$)
I	0.0	20.5	80.5	7.1
	12.5	11.8	108	5.8
	25.0	7.2	86.5	5.4
	50.0	3.8	68.4	4.6
II	0	26.7	131	10.5
	2	22.9	134	9.9
	6	20.0	153	8.1
	18	13.1	156	6.8
	60	5.6	140	6.1

Experiment		V ($\mu\text{M}/\text{sec}$)	K_s (μM)	K_{i1} (μM)	K_{i2} (μM)
I	pooled data	20.1	83.4	12.1	13.0
II	pooled data	23.4	138	13.9	10.8

The kinetic parameters V_{\max} , K_m and const. were obtained by fitting eqn 2 to substrate velocity data obtained at each papaverine concentration as described in Materials and Methods. The parameters K_s , V , K_{i1} , K_{i2} were calculated by fitting eqn 3 to the pooled data of an individual experiment after subtraction of the unsaturable flux components measured at each papaverine concentration.

Acknowledgement—This study has been supported by the “Anton-Dreher Gedächtnisschenkung für Medizinische Forschung”, Grant No. 95/87.

REFERENCES

1. Plagemann PGW and Wohlhueter RM, Permeation of nucleosides, nucleic acid bases, and nucleotides in animal cells. *Curr Top Membr Transp* **14**: 255–330, 1980.
2. Wohlhueter RM and Plagemann PG, The roles of transport and phosphorylation in nutrient uptake in cultured animal cells. *Int Rev Cytol* **64**: 171–240, 1980.
3. Müller MM, Kraupp M, Chiba P and Rumpold H, Regulation of purine uptake in normal and neoplastic cells. *Adv Enzyme Regul* **21**: 239–256, 1983.
4. Lönn U, Lönn S, Nylen U and Winblad G, 5-fluoropyrimidine-induced DNA damage in human colon carcinoma and its augmentation by the nucleoside transport inhibitor dipyridamole. *Cancer Res* **49**: 1085–1089, 1989.
5. Kang G-J and Kimball AP, Dipyridamole enhancement of toxicity to L1210 cells by deoxyadenosine and deoxycytosine combinations *in vitro*. *Cancer Res* **44**: 461–466, 1984.
6. Marz R, Wohlhueter RM and Plagemann PGW, Growth rate of cultured novikoff rat hepatoma cells as a function of the rate of thymidine and hypoxanthine transport. *J Memb Biol* **34**: 277–288, 1977.
7. Gaffen JD, Chambers EA and Bennett A, The effects of dipyridamole and indomethacin on methotrexate cytotoxicity in lovo human colon cancer cells. *J Pharm Pharmacol* **41**: 350–352, 1989.
8. Cabral S, Leis S, Bover L, Nembrot M and Mordoh J, Dipyridamole inhibits reversion by thymidine of methotrexate effect and increases drug uptake in sarcoma 180 cells. *Proc Natl Acad Sci USA* **81**: 3200–3203, 1984.
9. Chan T and Howell SB, Mechanism of synergy between *N*-phosphonacetyl-L-aspartate and dipyridamole in a human ovarian carcinoma cell line. *Cancer Res* **45**: 3598–3604, 1985.
10. Plagemann PG and Kraupp M, Inhibition of nucleoside and nucleobase transport and nitrobenzylthioinosine binding by dilazep and hexobendine. *Biochem Pharmacol* **35**: 2559–2567, 1986.
11. Chan T, Augmentation of 1-beta-arabinofuranosyl-cytosine cytotoxicity in human tumor cells by inhibiting drug efflux. *Cancer Res* **49**: 2656–2660, 1989.
12. Griffith DA and Jarvis SA, High affinity sodium-dependent nucleobase transport in cultured renal epithelial cells (LL-PK₁). *J Biol Chem* **268**: 20085–20090, 1993.
13. Domin BA, Mahony WB and Zimmerman TP, Purine nucleobase transport in human erythrocytes. *J Biol Chem* **263**: 9276–9284, 1988.
14. Kraupp M, Marz R, Prager G, Kommer W, Razavi M, Baghestanian M and Chiba P, Adenine and hypoxanthine transport in human erythrocytes: Distinct substrate effects on carrier mobility. *Biochim Biophys Acta* **1070**: 157–162, 1991.
15. Plagemann PG and Wohlhueter RM, Hypoxanthine transport in mammalian cells: cell type-specific differences in sensitivity to inhibition by dipyridamole and uridine. *J Memb Biol* **81**: 255–262, 1984.
16. Plagemann PGW, Wohlhueter RM and Woffendin C, Nucleoside and nucleobase transport in animal cells. *Biochim Biophys Acta* **947**: 405–443, 1988.
17. Gati WP, Paterson ARP, Tyrell DLJ, Cass CE, Moravsek J, and Robins MJ, Nucleobase transporter-mediated permeation of 2',3'-dideoxyguanosine in human erythrocytes and human T-lymphoblastoid CCRF-CEM cells. *J Biol Chem* **267**: 22272–22276, 1992.
18. Mahony WB, Domin BA, McConnell RT and Zimmerman TP, Acyclovir transport into human erythrocytes. *J Biol Chem* **263**: 9285–9291, 1988.
19. Coffman JD, Vasodilator drugs in peripheral vascular disease. *Am J Hosp Pharm* **32**: 1276–1281, 1975.
20. Sixma JJ, Holmsen H and Trieschnigg ACM, Adenine nucleotide metabolism of blood platelets. Transport of adenine into human platelets. *Biochim Biophys Acta* **443**: 33–48, 1973.
21. Plagemann PG and Wohlhueter RM, Inhibition of the transport of adenosine, other nucleosides and hypoxanthine in novikoff rat hepatoma cells by methylxanthines, papaverine, N⁶-cyclohexyladenosine and N⁶-phenylisopropyladenosine. *Biochem Pharmacol* **23**: 1783–1788, 1984.
22. Wohlhueter RM, Marz R, Graff JC and Plagemann PGW, A rapid-mixing technique to measure transport in suspended animal cells: applications to nucleoside transport in novikoff rat hepatoma cells. *Methods Cell Biol* **20**: 211–236, 1978.
23. Bevington PR, *Data Reduction and Error Analysis for the Physical Sciences*. McGraw-Hill, New York, 1969.
24. Plagemann PGW, Woffendin C, Puziss MB and Wohlhueter RM, Purine and pyrimidine transport and permeation in human erythrocytes. *Biochim Biophys Acta* **905**: 17–29, 1987.
25. Devés R and Krupka RM, Inhibition kinetics of carrier systems. *Methods Enzymol* **171**: 113–132, 1989.